
Synthesis and photocatalytic effects of TiO₂-Ag on antibiotic-resistant bacteria

Síntese e efeito fotocatalítico de TiO₂-Ag em bactérias resistentes a antibióticos

Iracema Nascimento de Oliveira¹, Raphaella Ingrid Santana Oliveira^{1*}, Eduarda Bezerra Pereira², Francine Ferreira Padilha¹, Silvia Maria Egues¹, Maria Lucila Hernández-Macedo^{1*}

ABSTRACT

Titanium dioxide (TiO₂) is a semiconductor metal oxide extensively studied due to its photocatalytic properties that can be applied in various areas. However, the catalytic performance of TiO₂ is limited at the UV spectrum, and the silver doping to titanium dioxide (Ag-TiO₂) can increase the catalytic performance for visible light. In this work, Ag-doped TiO₂ nanoparticles were synthesized to evaluate photocatalytic activity against sensitive and methicillin-resistant *Staphylococcus aureus* frequently associated with skin infections. The sol-gel method followed by Ag doping was applied to NPs synthesis. NPs were characterized by UV-vis spectroscopy, scanning electron microscopy (SEM), UV-vis diffuse reflectance spectrophotometry (DRS), Semi-quantitative energy dispersive spectroscopy (EDS) and Fourier transform infrared (FTIR) spectroscopy. FTIR and EDS results confirmed the doping of silver in TiO₂. MEV analysis evidenced spherical nanoparticles between 8.5 - 25.6 nm. The TiO₂ nanoparticles combined with silver improved the antimicrobial effect of TiO₂ under visible light at 180 min, however, the greatest antimicrobial effect was observed under UV light at 120 min.

Keywords: TiO₂-Ag; Photocatalysis; UV; Visible light; MRSA.

RESUMO

O dióxido de titânio (TiO₂) é um óxido metálico semicondutor amplamente estudado devido às suas propriedades fotocatalíticas que podem ser aplicadas em diversas áreas. No entanto, o desempenho catalítico do TiO₂ é limitado no espectro UV, e a dopagem com prata (Ag-TiO₂) pode aumentar seu desempenho em luz visível. Neste trabalho, foram sintetizadas nanopartículas de TiO₂ dopadas com Ag para avaliar a atividade fotocatalítica contra *Staphylococcus aureus* sensível e resistente à metilina frequentemente associado a infecções cutâneas. O método sol-gel seguido de dopagem com Ag foi aplicado para a síntese de NPs. As NPs foram caracterizadas por espectroscopia UV-Vis, microscopia eletrônica de varredura (SEM), espectrofotometria de refletância difusa UV-Vis (DRS), espectroscopia semi-quantitativa de energia dispersiva (EDS) e espectroscopia de infravermelho por transformada de Fourier (FTIR). Os resultados de FTIR e EDS confirmaram a dopagem da prata em TiO₂. A análise MEV evidenciou nanopartículas esféricas entre 8.5 - 25.6 nm. As nanopartículas de TiO₂ combinadas com prata melhoraram o efeito antimicrobiano do TiO₂ sob luz visível aos 180 min, no entanto, o maior efeito antimicrobiano foi observado sob luz UV aos 120 minutos.

Palavras chaves: TiO₂-Ag; Fotocatálise; UV; Luz Visível; SARM.

¹ Tiradentes University.

*E-mail: dr.raphaella@gmail.com

*E-mail: lucyherma@gmail.com

² Federal University of Sergipe.

INTRODUCTION

Nanoparticles (NPs) are materials whose dimensions permeate at a nanometric scale smaller than 100 nm (LAURENT et al., 2008). Due to its physical-chemical characteristics, versatility, and the advent of biotechnology, NPs play an increasing role in applications in several industrial fields from nanotechnology to biomedical. Nanomaterials synthesized from metallic oxides (MO), were mainly applied to promote the increase in investment for research on these materials in the last decade (KHAN; SAEED; KHAN, 2019; LIMO et al., 2018).

Titanium dioxide (TiO_2) is a MO found in nature in the forms of anatase, brookite, and rutile. Anatase exhibits the most stable polymorph with the highest electron mobility at a wide band gap of 3.2 eV (GUPTA; TRIPATHI, 2011; RATHORE et al., 2021). The wide band gap of anatase leads to its activation of electrons under ultraviolet (UV) light, which limited its photocatalytic activity under visible light (3-5%) (HU et al., 2010). The formation of hybrid NPs by combining TiO_2 with other semiconductors, redox couples, organic sensitizers or metal NPs is an alternative, since they can improve the visible light spectrum action by decreasing the band-gap, thus it is widely used for the photocatalysts production by improving activity under visible light (TRUPPI et al., 2017). Among the most used metals to reduce the band-gap energy are Ag, Cu, Fe, which, in addition to increasing the photocatalytic effect of TiO_2 , also have antimicrobial properties (GOPINATH et al., 2016; ZHANG et al., 2018).

The use of Ag to reduce the TiO_2 band gap is justified because Ag exhibits the phenomenon of surface plasmon resonance (SPR) in silver nanoparticles (AgNP) (PETRONELLA et al., 2019). The intense plasmonic bands of AgNP are active under visible light, so when electromagnetic radiation falls on its surface there is an oscillation of electrons, making it a good material for combining with the surface of TiO_2 . In addition, the band-gap reduction of TiO_2 could increase the amount of silver for doping which results in a greater capacity of TiO_2 to absorb visible light (SEERY et al., 2007).

The photo-activated propriety in TiO_2 ensures a key role in environmental remediation, effluent treatment, self-cleaning surfaces, solar fuels, and photovoltaic energy, as well as in the biomedical sector. In the biomedical field, TiO_2 was applied in antibacterial activities, and treatment of neoplastic cells, although the mechanism of its photobiological action is still not well known (LIMO et al., 2018; MENDES et al., 2020; RIBEIRO; FERRARI; TAVARES, 2020).

On the other hand, silver nanoparticles (AgNPs) have antimicrobial properties and are used for coatings and disinfection of medical devices, and water purification, showing its diverse applicability (PEIRIS et al., 2017). In this context, the development of new antimicrobial agents is relevant due to the ability of microorganisms, mainly bacteria, to become resistant to drugs available (HAIDER; JAMEEL; AL-HUSSAINI, 2019). The literature reports the antimicrobial drugs resistance in numerous pathogens, and the most frequently cited microorganisms are the bacteria *Staphylococcus aureus* and *Pseudomonas aeruginosa* and the fungus *Candida albicans*, all of which are often involved in nosocomial infections (BERKOW; LOCKHART, 2017; SOUZA et al., 2019).

Considering that TiO₂-Ag has photocatalytic action, this nanoparticle can act against microorganisms related to skin infections. Skin and soft tissue infections are often caused by microorganisms called ESKAPE (*Enterococcus faecium*, *Staphylococcus aureus*, *Klebsiella pneumoniae*, *Acinetobacter baumannii*, *Pseudomonas aeruginosa*, and *Enterobacter* sp.), with *S. aureus* and *P. aeruginosa* being the most commonly isolated from wounds chronicles (PFALZGRAFF; BRANDENBURG; WEINDL, 2018). *Staphylococcus aureus* is extremely virulent gram-positive cocci, known to produce several toxins, responsible for variable infectious conditions. According to Thurlow et al. (2018), skin and soft tissue infections are the clinical presentation most commonly associated with methicillin-resistant *S. aureus* (MRSA). Another gram-positive bacterium, *Streptococcus pyogenes*, is also constantly related to skin infections such as necrotizing fasciitis, this pathology is characterized by tissue failure reaching the fascia and soft tissues, which can occur after the loss of skin integrity and spread through the hematogenic (NEILLY et al., 2019).

Studies show the metallic NPs effects in numerous microbial species such as viruses, bacteria, fungi, and protozoa (BOXI; MUKHERJEE; PARIA, 2016; MOONGRAKSATHUM; CHIEN; CHEN, 2019). Therefore, in the last decades, TiO₂ was the most explored photocatalyst material for its low cost and physical-chemical properties (HAMPEL et al., 2020; WANG et al., 2012). The combination of TiO₂-Ag exhibited photocatalytic activity against biofilm and planktonic bacterial of various microbial agents (D et al., 2011; MARTINEZ-GUTIERREZ et al., 2010; WANG et al., 2016). In this work, the photocatalytic activity of synthesized TiO₂ nanoparticles and Ag-

doped TiO₂ were investigated by comparison of doping Ag to commercial TiO₂ nanoparticles (Degussa P25).

MATERIAL AND METHODS

Synthesis of pure TiO₂ nanoparticles

The material synthesis was carried out by the described Jagadale et al. (2008) methodology. For the procedure, 30 mL of ethyl alcohol was added to a beaker followed by 15.6 mL (by drop) of titanium tetra isopropyl precursor (TTIP, 97%, Aldrich), and the mixture was subjected to constant magnetic stirring. After that, 150 mL of distilled water was added, keeping the mixture under stirring for 10 min. After homogenization, the material was covered by aluminum foil for decanting at room temperature for 48 h. After this period, the water was carefully removed with the aid of a syringe, and the decanted material was washed with 500 mL of distilled water and filtered with a vacuum pump. The mass obtained was dried in an oven at 38 °C for 72 h. After drying, the material was calcined at 400 °C in a muffle to get the anatase form (GUPTA; TRIPATHI, 2011). The procedure was performed on a ramp at 105 °C for 30 min, with a heating rate of 5 °C/min, followed at 400 °C for 120 min, using a muffle (Q318M24 Quimis). The samples were cooled in the muffle for 24 h.

TiO₂ doping with Ag

The TiO₂ doping with Ag was performed using TiO₂ synthesized and commercial TiO₂ (Degussa P25) NPs. The TiO₂ nanoparticles (5 g) were submitted to an ultrasonic bath for 1 h, then, under stirring was added 30 mL of AgNO₃ (0.5 M) (Ag⁺ 3% w/w). After 30 min was added 120 mL of the reducing agent sodium formate at 0.15 M. The samples remained under light protection and in constant stirring for 4 h, followed by decantation for 12 h. After the particle's sedimentation, the material was washed with distilled water, followed by vacuum pump filtration.

Nanoparticles characterization

The analysis of the nanoparticle's optical proprieties was performed by UV–vis diffuse reflectance spectra (UV-DRS), using a Shimadzu spectrophotometer, model UV-2600 in the range from 200 nm to 800 nm. The surface morphology and size of NPs were characterized using scanning electron microscopy (SEM) coupled to energy dispersive

spectroscopy (EDS) model JOEL JSM-IT200. EDS analysis was performed after image analysis to detect Ag- TiO₂ conjugation. The measures of the hydrodynamic diameter of nanoparticles in solution were evaluated by dynamic light scattering (DLS) using Malvern Zetasizer (Malvern Zetasizer) equipment. The conjugation of Ag- TiO₂ was analyzed by attenuated total reflectance Fourier-transform infrared spectroscopy (ATR-FTIR) in the range 4000-600 cm⁻¹ and 2 cm⁻¹ of resolution, using the *Cary 630 FTIR* spectrometer (Agilent Technologies, USA).

Antibacterial activity

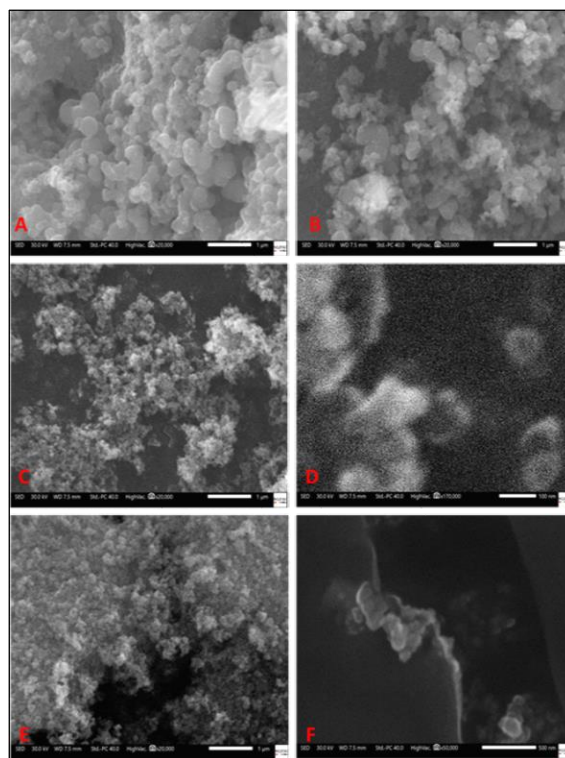
The photocatalytic potential of nanoparticles on bacteria was evaluated following the methodology described by Yadav et al. (2014), using a fluorescent lamp (Philips 8WWW T5, $\lambda > 400$ nm) and UV lamp (Philips 8W BLB T5, $\lambda = 365$ nm) with light intensity at $\sim 0,5$ mW cm⁻². Bacterial strains *Staphylococcus aureus* ATCC 25923 INCQS 00015 and *Staphylococcus aureus* ATCC 43300 INCQS 00577 (methicillin-resistant) were used for the antimicrobial test. Bacteria were grown on Brain Heart Infusion broth (BHI) for 24 h at 37 °C and then, bacterial suspensions (10⁸ CFU/mL) in saline solution determined according to the 0.5 McFarland scale were prepared. 1 mg/mL of TiO₂ NPs suspension, previously sonicated was prepared and added to bacterial suspensions at 0.5 McFarland scale. The sample of the NPs with the bacteria was submitted to the photocatalytic test under dark, visible light, and UV light conditions at 60, 120, and 180 min. After photocatalytic treatment, irradiated samples (10 μ L) were inoculated in triplicate into sterile 96-well polystyrene microplates containing 2 \times concentrated BHI broth (100 μ L). As a blank, 2 \times concentrated BHI broth (100 μ L) and TiO₂ NPs (10 μ L) were used. As growth control, 2 \times concentrated BHI (100 μ L) and bacterial inoculum (10⁸ CFU/mL) (10 μ L) were used, and ultrapure water was used as a negative control. BHI broth 2 \times concentrate (100 μ L) was used for experimental sterility control. The plates were incubated at 37 °C for 24 h and bacterial viability was revealed using 20 μ L of the developer 2,3,5 Triphenyl Tetrazolium Chloride (TTC) (Dinâmica®, Diadema, São Paulo) 0.5% (w/v) in ultrapure water for 2 h. After treatment, the viability of microorganisms was assessed by absorbance at 595 nm using a microplate reader (Biochrom EZ Read 2000).

RESULTS AND DISCUSSION

Synthese and TiO₂ doping and nanoparticles characterization

The white precipitate observed during NPs synthesis and the color change of the solution when added AgNO₃ and sodium formate suggests obtaining TiO₂ NPs. These characteristics corroborate with the results of Vijayalakshmi et al. (2015), who obtained pure nanoparticles in anatase form. The pure TiO₂ synthesized nanoparticle exhibited an average size of 25.6 nm +/- 9.6 (Figure 1A) while the Ag-doped TiO₂ had an average size of 22 nm +/- 5 (Figure 1B). Figures 1C and 1D show commercial TiO₂ NPs (Degussa P25) with a size of 8.5 nm. Figures 1E and 1F show commercial TiO₂ samples doped with Ag with a size of 11.1 nm. In TiO₂ Degussa P25 doped with silver samples, it was not possible to calculate the arithmetic average and standard deviation, due to the difficulty of obtaining the precise size of the material since the size of the nanoparticles was very close to the microscope reach limit.

Figure 1: Scanning electron microscopy (SEM); nanoparticles of synthesized TiO₂ (A), synthesized TiO₂-Ag (B), TiO₂ P25 (C and D), TiO₂Ag P25 (E and F).

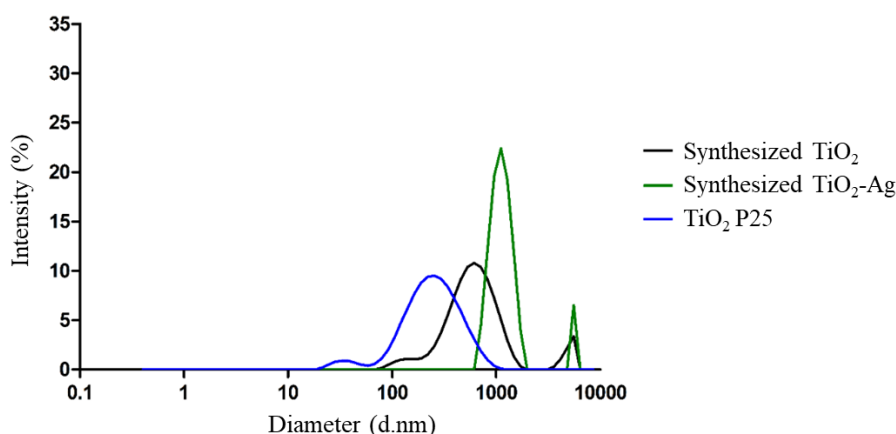


Fonte: Aatoria propria (2023)

According to dynamic light scattering (DLS) analyses (Figure 2), the distribution curve of nanoparticle analyses suggests that the materials formed agglomerates, which

probably led to their rapid sedimentation during the sample processing. Nanoparticles in suspension showed a variable degree of agglomeration and hydrodynamic diameter, as shown in Table 1. In the sample of commercial TiO₂ (P25) doped with silver, the formation of intensity curve by diameter was not observed, probably due to the high agglomeration of this material, generating results on a larger scale, not detected by the technique.

Figure 2: Dynamic light scattering (DLS) of synthesized TiO₂ nanoparticles, synthesized TiO₂-Ag, and TiO₂ P25 (comercial).



Fonte: Aatoria própria (2023)

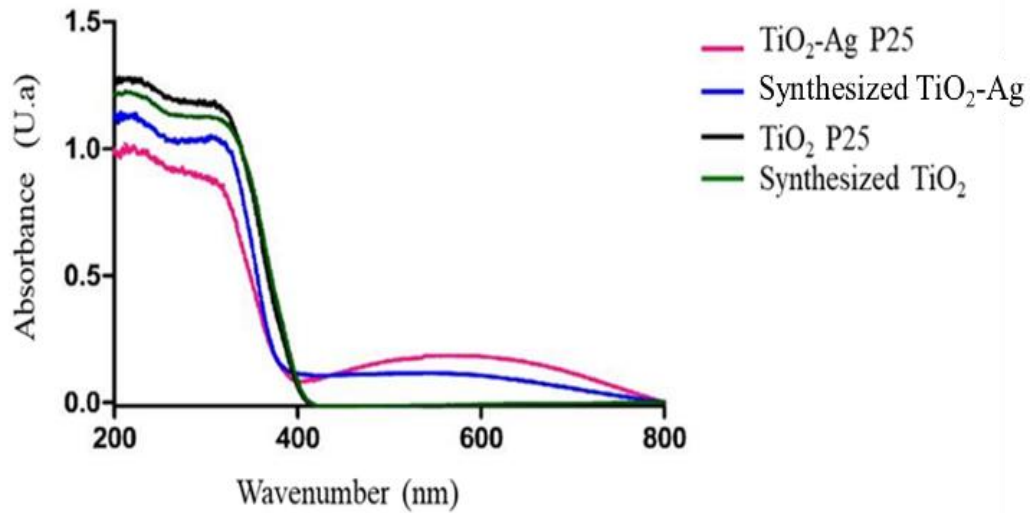
Table 1: Size hydrodynamic diameter variation of NPs by DLS.

Material	Variation in Diameter (d.mn)
TiO ₂ P25	19,9- 8.939
Synthesized TiO ₂	0,4-64.40
Synthesized TiO ₂ -Ag	0,4-8.630

Fonte: Aatoria própria (2023)

The NPs under UV and VIS light spectrum performance were evaluated by DRS. This analysis showed that the TiO₂-Ag sample has a range of absorption between 400 and 750 nm, which corresponds to the visible region. Spectra in the visible region were not observed in pure TiO₂ P25 samples (Figure 3).

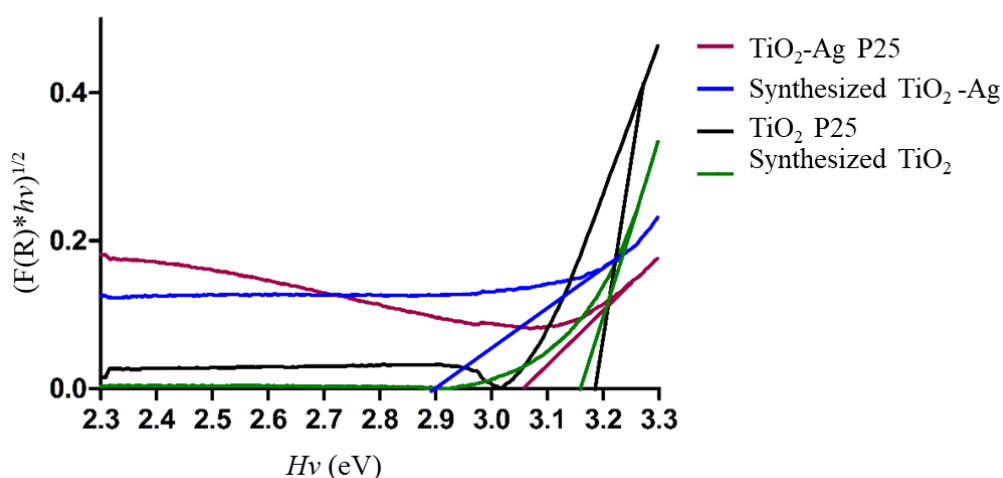
Figure 3: UV-Vis diffuse reflectance spectrophotometry (DRS) of TiO₂-Ag P25, synthesized TiO₂-Ag (3% (w/w) Ag⁺: TiO₂), commercial TiO₂ P25, and synthesized TiO₂ samples.



Fonte: Autoria própria (2023)

The band gap was also calculated using according to the Kubelka-Munk function (KHAN et al., 2014) (Figure 4). The band-gap values of synthesized TiO₂, TiO₂ Degussa P25, and TiO₂-Ag Degussa P25 were similar (3.16, 3.19, and 3.05 respectively). The smallest band gap that indicates the greatest photocatalytic capacity was observed in the synthesized TiO₂-Ag NP (2.9 Hv (eV)) (Table 2).

Figure 4: Band gap energy of TiO₂ P25-Ag, TiO₂-Ag (3% (w/w) Ag⁺: TiO₂), commercial TiO₂ P25, and synthesized TiO₂ samples.



Fonte: Aatoria própria (2023)

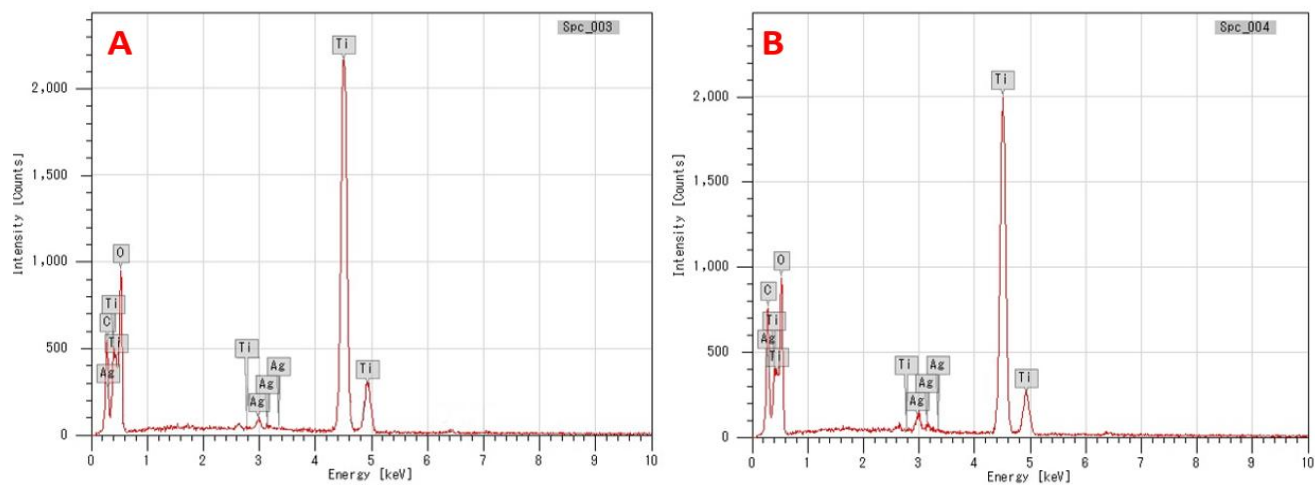
Table 2: Band gap energy values of the nanoparticles.

Material	Band-gap $H\nu$ (eV)
Synthesized TiO ₂	3.16
TiO ₂ Degussa P25	3.19
Synthesized TiO ₂ -Ag	2.9
TiO ₂ -Ag Degussa P25	3.05

Fonte: Aatoria própria (2023)

The analysis by EDS confirmed that silver-doped nanoparticles are composed of titanium, oxygen, and silver molecules (Figure 6A and 6B). The chemical elements present in these nanoparticles were also evaluated according to their proportions (Table 3 and Table 4). Thus, the synthesized TiO₂-Ag (2.59 %) showed higher silver doping in its structure when compared to the commercial TiO₂-Ag P25 (1.4%). This result confirms that greater doping of Ag to TiO₂ reduces the band gap (Figure 4), increasing the absorption of the photocatalyst under visible light, as also observed by (SEERY et al., 2007).

Figure 6: Energy dispersive spectroscopy (EDS) spectrum of synthesized TiO₂-Ag (A) and TiO₂-Ag P25 commercial (B).



Fonte: Autorial própria (2023)

Table 3: Energy dispersive spectroscopy (EDS) analysis of the chemical elements of TiO₂-Ag P25 sample.

Element	% Mass	% Atomic
C	14.16±0.13	23.9±0.23
O	44.87±0.60	58.58±0.79
Ti	39.54±0.31	17.24±0.13
Ag	1.43±0.08	0.28±0.02
Total	100.00	100.00

Fonte: Autorial própria (2023)

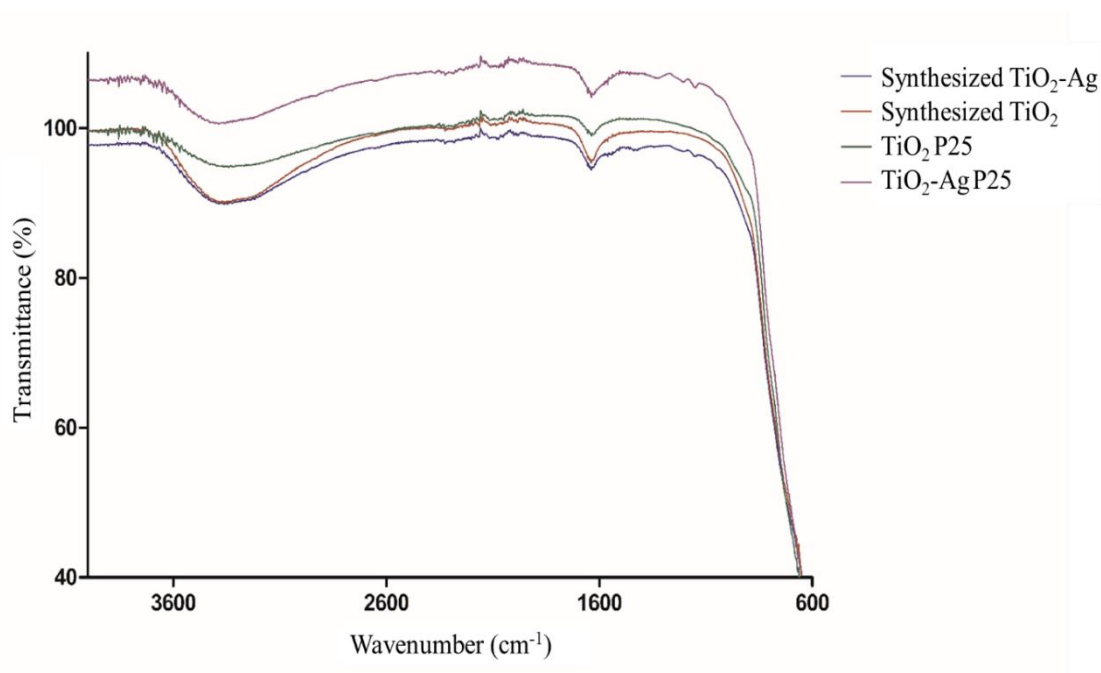
Table 4: Energy dispersive spectroscopy (EDS) analysis of the chemical elements in the synthesized TiO₂-Ag.

Element	% Mass	% Atomic
C	18.07 ±0.15	30.02±0.25
O	43.92 ±0.60	54.76±0.75
Ti	35.41±0.29	14.75±0.12
Ag	2.59±0.10	0.48±0.02
Total	100.00	100.00

Fonte: Autorial própria (2023)

FTIR analyses were performed to verification of the chemical groups in the nanoparticles (Figure 7). Bands in the region around 3500 to 3000 cm^{-1} are attributed to the hydroxyl groups –OH vibration was observed (HERNÁNDEZ ENRÍQUEZ et al., 2008; VIJAYALAKSHMI et al., 2015), while the bands around 1600 cm^{-1} are derived from O-H deformation of water adsorbed on the NP surface (GUERRERO et al., 2015; LIU et al., 2013). According to Ali et al. (2018), the presence of the hydroxyl group plays a fundamental role for improving the photocatalytic activity due to the action of OH groups to remove electrons and photogenerated holes. Bands smaller than 1000 cm^{-1} are expected in O–Ti–O vibrations, which are attributed to the formation of TiO_2 (GUERRERO et al., 2015; VIJAYALAKSHMI et al., 2015). In synthesized TiO_2 -Ag and commercial TiO_2 -Ag, bands were observed at 3.421 cm^{-1} which refer to Ag vibrations (GHOSH et al., 2020), confirming the doping of Ag to TiO_2 .

Figure 7: Fourier transform infrared spectroscopy (FTIR) of commercial TiO_2 (P25), and synthesized pure and doping Ag.



Fonte: Aatoria própria (2023)

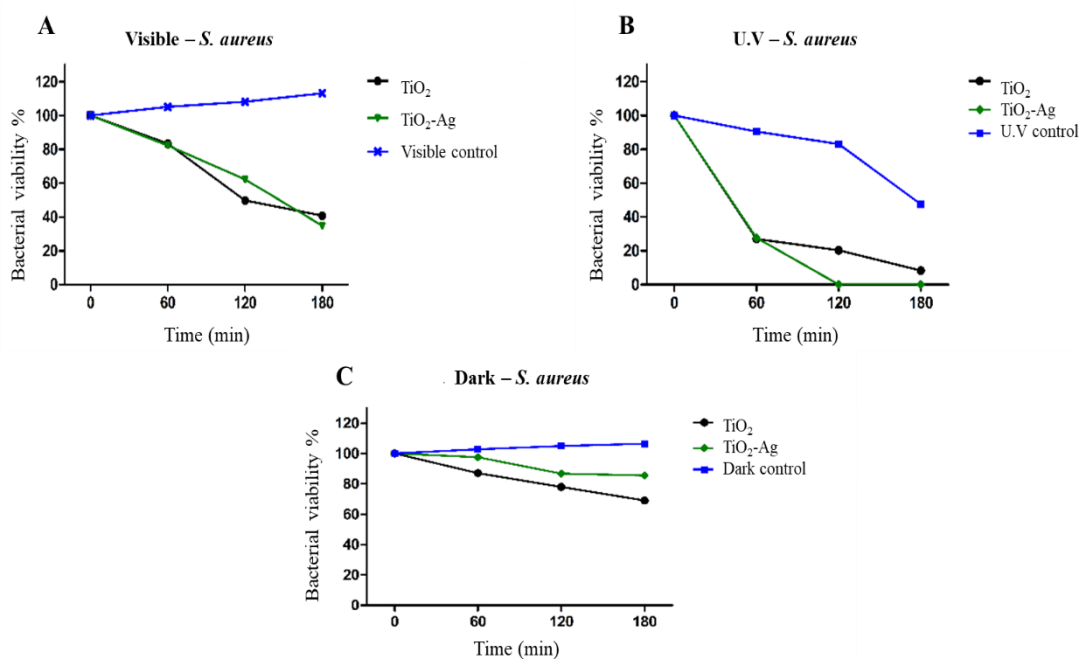
Antibacterial activity

The pure synthesized TiO_2 and doping with Ag were applied for the antibacterial test by photocatalysis (Figure 8). The choice for antimicrobial analysis of the synthesized photocatalysts was based on the low band gap values of these materials (Table 2). The

results were carried out under visible light, UV light and dark conditions at 60, 120 and 180 on bacteria *S. aureus* ATCC 25923 (antibiotic sensitive) and *S. aureus* ATCC 43300 (methicillin resistant).

The analysis with *S. aureus* (antibiotic sensitive) under visible light showed a reduction in bacterial viability of 40.79% and 34.81%, respectively after 180 min with TiO₂ and TiO₂-Ag NPs, evidencing the bacteriostatic potential of these photocatalysts under these conditions (Figure 8A). Under UV light conditions, a bacterial viability reduction at 47% was observed in the control sample (without photocatalysts) (Figure 8B). However, a viability reduction lower than the control was observed with NPs synthesized: 8.31% in the TiO₂ treatment at 180 min and total bacteria inhibition with TiO₂-Ag at 120 min, showing the bacteriostatic and bactericidal effect of these NPs, respectively (Figure 8B). In the dark condition (Figure 8C), a moderate decrease in the bacteria viability of 69.08% and 85.56% was observed in treatment with TiO₂ and TiO₂-Ag, respectively, which suggests the toxicity of NPs without photocatalysis.

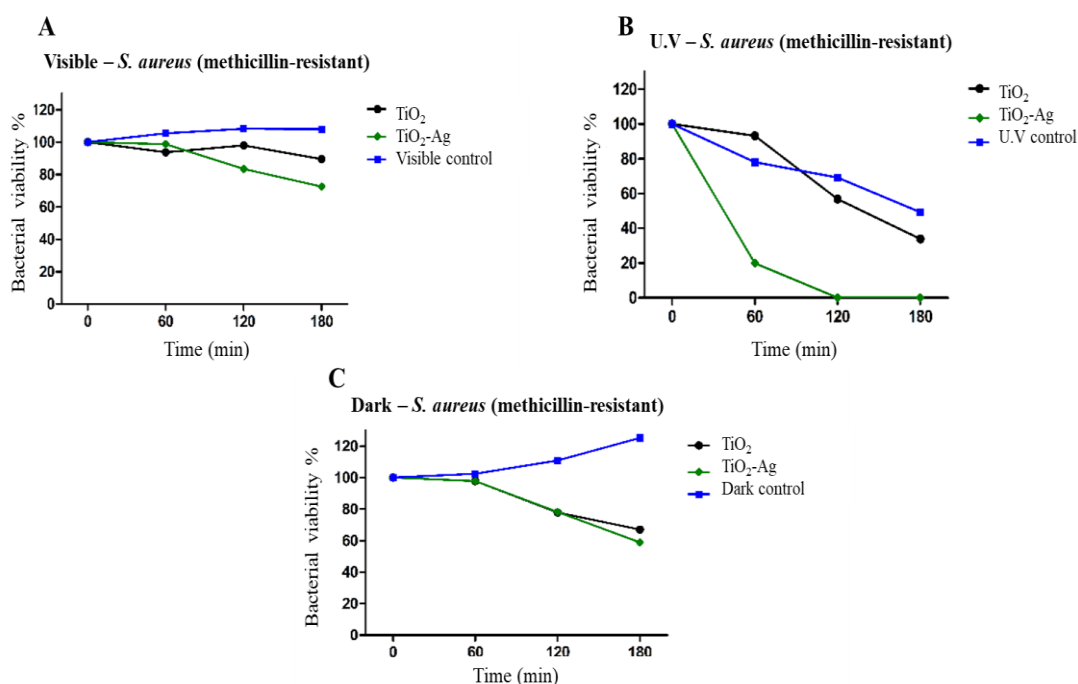
Figure 8: Viability of methicillin-sensitive *S. aureus* exposed to photocatalysis with TiO₂ and TiO₂-Ag under visible light (A), UV light (B), and dark (C) conditions.



Fonte: Autoria própria (2023)

The photocatalyst assays with methicillin-resistant *S. aureus* showed that under visible light conditions, the bacterium has a high viability of 89.52% with TiO₂ and 72.56% with TiO₂-Ag at 180 min (Figure 9A). These values indicate that this strain is more resistant to photocatalysis with nanoparticles under visible light when compared to methicillin-sensitive *S. aureus* (Figure 8A). Under UV light treatment (Figure 9B), the results showed a bacterial viability of 33.82% with TiO₂ treatment at 180 min while cellular invariability was observed with TiO₂-Ag NP at 120 min. Thus, under UV conditions the photocatalytic NPs activity was similar to the methicillin-sensitive strain (Figure 8B) this suggests that UV light increases the photocatalytic potential of the nanoparticles. The results under dark conditions also show a reduction in the microbial viability in 66.96% with TiO₂ NP and 58.88% with TiO₂-Ag NP (Figure 9C).

Figure 9: Viability of methicillin-resistant *S. aureus* exposed to photocatalysis with TiO₂ and TiO₂-Ag under visible light (A), UV light (B), and dark (C) conditions.



Fonte: Autoria própria (2023)

From the antimicrobial experiment by photocatalysis, a greater photocatalytic performance was shown in the treatment under UV light with total bacterial inhibition at 120 min. Under visible light, the photocatalysts were less efficient against the resistant strain when compared to the sensitive strain. This result can be explained by the UV

radiation itself having antimicrobial activity and by the low nanoparticles photocatalytic performance in the visible light spectrum observed in the DRS-UV-Vis analysis. A decrease in bacterial growth was also observed under dark conditions, suggesting the toxicity of NPs on the microorganisms.

CONCLUSION

Nanoparticles of TiO₂ and TiO₂ doped with Ag were obtained, and this doping improves the light absorption of samples in the visible region as demonstrated in DRS-UV-Vis analysis. The nanoparticles had an average size between 8.5 nm and 25.6 nm and a spherical shape, desirable characteristics for antimicrobial nanomaterials since the nanoparticle's size and shape result in the influence of the microorganism interaction. The silver doping to TiO₂ was confirmed by the analysis of EDS and FTIR, however, the nanoparticles tended to agglomerate which could interfere with their interaction with the bacterial cell wall. Despite the characterization results showing improved light absorption under the visible spectrum, the antimicrobial tests showed better photocatalytic activity under the UV light spectrum. This occurs probably due to the inherent antimicrobial ability of the UV radiation and also the amount of Ag in TiO₂. Although bacterial inhibition was observed under UV light, silver doping of TiO₂ decreased the inhibition time from 180 min to 120 min. Thus, the NPs' activity for antimicrobial purposes shows the potential of these nanomaterials for in vivo photocatalytic tests.

ACKNOWLEDGMENT

The authors thank the funding National Council for Scientific and Technological Development- CNPq (Grant: 01/2019-PIBIC, 305462/2021-0 DT2 and, 313662/2019-3 DT2), Coordination for the Improvement of Higher Education Personnel (CAPES) (Grant:001) and Foundation for Research and Technological Innovation Support of the State of Sergipe (FAPITEC/SE) for financial support and student fellowship.

REFERENCES

- ALI, T. et al. Enhanced photocatalytic and antibacterial activities of Ag-doped TiO₂ nanoparticles under visible light. **Materials Chemistry and Physics**, v. 212, p. 325–335, 2018.
- BERKOW, E. L.; LOCKHART, S. R. Fluconazole resistance in *Candida* species: a current perspective. **Infection and Drug Resistance**, v. 10, p. 237–245, 2017.

BOXI, S. S.; MUKHERJEE, K.; PARIA, S. Ag doped hollow TiO₂ nanoparticles as an effective green fungicide against *Fusarium solani* and *Venturia inaequalis* phytopathogens. **Nanotechnology**, v. 27, n. 8, p. 085103, 2016.

D, B. et al. Nanostructured TiO₂ and TiO₂-Ag antimicrobial thin films. **TechConnect Briefs**, v. 3, n. 2011, p. 271–274, 2011.

GHOSH, M. et al. Enhanced photocatalytic and antibacterial activities of mechanosynthesized TiO₂-Ag nanocomposite in wastewater treatment. **Journal of Molecular Structure**, v. 1211, p. 128076, 2020.

GOPINATH, K. et al. Eco-friendly synthesis of TiO₂, Au and Pt doped TiO₂ nanoparticles for dye sensitized solar cell applications and evaluation of toxicity. **Superlattices and Microstructures**, v. 92, p. 100–110, 2016.

GUERRERO, V. et al. Síntesis y Caracterización de Nanopartículas de Dióxido de Titanio Obtenidas por el Método de Sol-Gel. **Revista Politécnica**, v. 36, p. 7–13, 2015.

GUPTA, S. M.; TRIPATHI, M. A review of TiO₂ nanoparticles. **Chinese Science Bulletin**, v. 56, n. 16, p. 1639–1657, 2011.

HAIDER, A. J.; JAMEEL, Z. N.; AL-HUSSAINI, I. H. M. Review on: Titanium Dioxide Applications. **Energy Procedia**, v. 157, p. 17–29, 2019.

HAMPEL, B. et al. Application of TiO₂-Cu Composites in Photocatalytic Degradation Different Pollutants and Hydrogen Production. **Catalysts**, v. 10, n. 1, p. 85, 2020.

HERNÁNDEZ ENRÍQUEZ, J. M. et al. Síntesis y caracterización de nanopartículas de N-TiO₂ - Anatasa. **Superficies y vacío**, v. 21, n. 4, p. 1–5, 2008.

HU, S. et al. Hydrothermal Synthesis of Well-dispersed Ultrafine N-Doped TiO₂ Nanoparticles with Enhanced Photocatalytic Activity under Visible Light. **Journal of Physics and Chemistry of Solids - J PHYS CHEM SOLIDS**, v. 71, p. 156–162, 2010.

KHAN, I.; SAEED, K.; KHAN, I. Nanoparticles: Properties, applications and toxicities. **Arabian Journal of Chemistry**, v. 12, n. 7, p. 908–931, 2019.

KHAN, M. M. et al. Band gap engineered TiO₂ nanoparticles for visible light induced photoelectrochemical and photocatalytic studies. **J. Mater. Chem. A**, v. 2, n. 3, p. 637–644, 2014.

LAURENT, S. et al. Magnetic Iron Oxide Nanoparticles: Synthesis, Stabilization, Vectorization, Physicochemical Characterizations, and Biological Applications. **Chemical Reviews**, v. 108, n. 6, p. 2064–2110, 2008.

LIMO, M. J. et al. Interactions between Metal Oxides and Biomolecules. 2018.

LIU, Y. et al. A comparison of N-doped TiO₂ photocatalysts preparation methods and studies on their catalytic activity: Comparison of N-doped TiO₂ photocatalyst preparation methods and activities. **Journal of Chemical Technology & Biotechnology**, v. 88, n. 10, p. 1815–1821, 2013.

MARTINEZ-GUTIERREZ, F. et al. Synthesis, characterization, and evaluation of antimicrobial and cytotoxic effect of silver and titanium nanoparticles. **Nanomedicine: Nanotechnology, Biology and Medicine**, v. 6, n. 5, p. 681–688, 2010.

MENDES, D. T. S. L. et al. Estudo da molhabilidade de nanotubos de TiO₂ incorporados com nanopartículas de Ag e ZnO / Study of the wetness of TiO₂ nanotubes incorporated with Ag and ZnO nanoparcales. **Brazilian Journal of Development**, v. 6, n. 10, p. 74439–74453, 2020.

MOONGRAKSATHUM, B.; CHIEN, M.-Y.; CHEN, Y.-W. Antiviral and Antibacterial Effects of Silver-Doped TiO₂ Prepared by the Peroxo Sol-Gel Method. **Journal of Nanoscience and Nanotechnology**, v. 19, n. 11, p. 7356–7362, 2019.

NEILLY, D. et al. Necrotising fasciitis in the North East of Scotland: a 10-year retrospective review. **The Annals of The Royal College of Surgeons of England**, v. 101, n. 5, p. 363–372, 2019.

PEIRIS, M. K. et al. Biosynthesized silver nanoparticles: are they effective antimicrobials? **Memórias do Instituto Oswaldo Cruz**, v. 112, n. 8, p. 537–543, 2017.

PETRONELLA, F. et al. Chapter 18 - Photocatalytic Application of Ag/TiO₂ Hybrid Nanoparticles. Em: MOHAPATRA, S.; NGUYEN, T. A.; NGUYEN-TRI, P. (Eds.). **Noble Metal-Metal Oxide Hybrid Nanoparticles**. Micro and Nano Technologies. [s.l.] Woodhead Publishing, p. 373–394, 2019.

PFALZGRAFF, A.; BRANDENBURG, K.; WEINDL, G. Antimicrobial Peptides and Their Therapeutic Potential for Bacterial Skin Infections and Wounds. **Frontiers in Pharmacology**, v. 9, p. 281, 2018.

RATHORE, N. et al. Optical, structural and morphological properties of Fe substituted rutile phase TiO₂ nanoparticles. **Physica B: Condensed Matter**, v. 600, p. 412609, 2021.

RIBEIRO, V. A. DOS S.; FERRARI, A. M.; TAVARES, C. R. G. Fotocatálise aplicada ao tratamento de efluentes de lavanderia de jeans: comparação entre TiO₂ e ZnO na eficiência de remoção de cor / Photocatalysis applied tolaundry wastewater treatment: comparison between TiO₂ and ZnO on the efficiency of color removal. **Brazilian Journal of Business**, v. 2, n. 3, p. 2788–2798, 2020.

SEERY, M. K. et al. Silver doped titanium dioxide nanomaterials for enhanced visible light photocatalysis. **Journal of Photochemistry and Photobiology A: Chemistry**, v. 189, n. 2–3, p. 258–263, 2007.

SOUZA, L. F. DE et al. Avaliação da Atividade Bacteriostática de Carvão Ativado Impregnado com Prata Frente à Bactéria *Pseudomonas aeruginosa*. **Revista Processos Químicos**, v. 13, n. 25, p. 71–78, 2019.

TRUPPI, A. et al. Visible-Light-Active TiO₂-Based Hybrid Nanocatalysts for Environmental Applications. **Catalysts**, v. 7, n. 4, p. 100, 2017.

VIJAYALAKSHMI, U. et al. Preparation and evaluation of the cytotoxic nature of TiO₂ nanoparticles by direct contact method. **International Journal of Nanomedicine**, p. 31, 2015.

WANG, H. et al. Au/TiO₂/Au as a Plasmonic Coupling Photocatalyst. **The Journal of Physical Chemistry C**, v. 116, n. 10, p. 6490–6494, 2012.

WANG, J. et al. Silver-nanoparticles-modified biomaterial surface resistant to staphylococcus: new insight into the antimicrobial action of silver. **Scientific Reports**, v. 6, n. 1, p. 32699, 2016.

YADAV, H. M. et al. Preparation and characterization of copper-doped anatase TiO₂ nanoparticles with visible light photocatalytic antibacterial activity. **Journal of Photochemistry and Photobiology A: Chemistry**, v. 280, p. 32–38, 2014.

ZHANG, X. et al. Effects of copper nanoparticles in porous TiO₂ coatings on bacterial resistance and cytocompatibility of osteoblasts and endothelial cells. **Materials Science and Engineering: C**, v. 82, p. 110–120, 2018.